Improvement of Biodistribution and Therapeutic Index *via* Increase of Polyethylene Glycol on Drug-carrying Liposomes in an HT-29/*luc* Xenografted Mouse Model

TONG-HSIEN CHOW[1], YI-YU LIN[1], JENG-JONG HWANG[1], HSIN-ELL WANG[1], YUN-LONG TSENG[2], SHYH-JEN WANG[3], REN-SHYAN LIU[3], WUU-JYH LIN[4], CHUNG-SHI YANG[5] and GANN TING[5]

[1]*Department of Biomedical Imaging and Radiological Sciences, National Yang-Ming University, Taipei;*
[2]*Taiwan Liposome Company, Taipei;*
[3]*Department of Nuclear Medicine, Taipei Veterans General Hospital, Taipei;*
[4]*Institute of Nuclear Energy Research, Lung-tan, Taoyuan;*
[5]*National Health Research Institute, Taipei, Taiwan, R.O.C.*

Abstract. *Liposomes modified with a high concentration of polyethylene glycol (PEG) could significantly prolong the retention time of the carried drug in the circulation, thus improving the drug accumulation in the tumor. In this study, 6 mol% rather than 0.9 mol% PEGylated liposomes (100 nm in diameter) encapsulated with indium-111 were used in a human colorectal carcinoma HT-29/luc tumor-bearing mouse model for comparing the PEGylation effect. Pharmacokinetics, biodistribution, passive-targeted assay, bioluminescence imaging (BLI) and tumor growth measurements were used for the spatial and temporal distribution, tumor localization and therapeutic evaluation of the drug. Pharmacokinetic studies indicated that the terminal half-life ($T_{1/2}\lambda z$) and C_{max} of 6 mol% PEG ^{111}In liposomes were similar to those of 0.9 mol% PEG ^{111}In liposomes. In the blood, the total body clearance (Cl) of 6 mol% PEG ^{111}In liposomes was about 1.7-fold lower and the area under the curve (AUC) was 1.7-fold higher than those of 0.9 mol% PEG ^{111}In liposomes. These results showed that the long-term circulation and localization of 6 mol% PEGylated liposomes was more appropriate for use in the tumor-bearing animal model. In addition, the biodistribution of 6 mol% PEG ^{111}In liposomes showed significantly lower uptake in the liver, spleen, kidneys, small intestine and bone marrow than those of 0.9 mol% PEG ^{111}In liposomes. The clearance rate of both drugs from the blood decreased with time, with the maximum at 24 h post intravenous (i.v.) injection. Prominent tumor uptake and the highest tumor/muscle ratios were found at 48 h post injection. Both AUC and relative ratio of the AUCs (RR-AUC) also showed that 6 mol% PEGylated liposomes significantly reduced the uptake of drugs in the reticuloendothelial system (RES), yet enhanced the uptake in the tumor. Gamma scintigraphy at 48 h post injection also demonstrated more distinct tumor uptake with 6 mol% PEG ^{111}In liposomes as compared to that of 0.9 mol% PEGylated liposomes ($p<0.01$). BLI and in vivo tumor growth tracing showed that growth in tumor volume could largely be inhibited by 6 mol% PEG ^{111}In liposomes. The results suggest that 6 mol% PEGylated liposomes might be a more suitable liposomal carrier for drug delivery than 0.9 mol% PEGylated liposomes, not only by reducing the drug accumulation in the RES or its related organs, but by prolonging drug circulation and eventually enhancing the targeting efficiency in the tumor to reach a better therapeutic index.*

Liposomes are polymeric nanoparticles which consist of one or more concentric phospholipid bilayers and are widely used as carriers for diagnostic and therapeutic agents (1-5). Liposomes comprise a promising drug delivery system owing to their slow drug release, and spatial and temporal distribution of drugs for targeted therapies. Liposomal carriers could be used to effectively encapsulate chemotherapeutic drugs for cancer therapy, antisense oligonucleotides for gene therapy, peptides for the treatment of infectious diseases, antigens to stimulate immune response, as well as radiopharmaceuticals for targeted imaging and radiotherapy (6-8). These encapsulated agents showed some improvement in pharmacokinetic stability, better biodistribution *i.e.* higher accumulation in target organs and lower normal tissue

Correspondence to: Jeng-Jong Hwang, Ph.D., Department of Biomedical Imaging and Radiological Sciences, National Yang-Ming University, No.155, Sec.2, Li-Nong St., Beitou, Taipei 112, Taiwan, R.O.C. Tel: +886 228267064, Fax: +886 228201095, e-mail: jjhwang@ym.edu.tw

Key Words: Polyethylene glycol, PEGylated liposome, reticuloendothelial system, indium-111, HT-29/*luc*, pharmacokinetics, biodistribution, bioluminescence imaging.

toxicity, and were delivered to areas which are usually inaccessible to non-encapsulated drugs. These properties have resulted in better therapeutic efficacy (9-11).

On the other hand, liposomes are also easily taken up by cells of the mononuclear phagocyte system (MPS) (12), primarily those located in the reticuloendothelial system (RES)-rich organs, such as liver, spleen and bone marrow. To overcome this problem, hydrophilic phosphatidylethanolamine (PE) derivatives of polyethylene glycol (PEG)-conjugated liposomes were initially developed to evade rapid liposomes clearance by the RES and ensure longer circulation of the drug for treatment (12, 13). PEGylated (*i.e.* coated with polyethylene glycol) liposomes exhibit their passive targeting property *via* the enhancement of permeability and retention (EPR) of nanoliposomes through leaky tumor vasculature in tumor xenografted animal models (6, 7, 14, 15). Pharmacokinetics and biodistribution of PEGylated liposomal formulations of doxorubicin (16-19) and daunorubicin (20, 21) have been applied to treat effectively against AIDS-related Kaposi's sarcoma (16, 22), ovarian (23), breast (24) and prostate cancer (25), and further gained regulatory approval for clinical use (26). Indium-111 has an appropriate half-life ($T_{1/2}$=67.9 h) and energy characteristics for diagnosis with gamma-ray imaging and in therapeutic strategies with Auger electrons. It has been demonstrated to be very efficient for tumor cell killing due to its extremely short, sub-cellular range (≤1 μm) with high linear energy transfer (LET) and relatively biological effectiveness (RBE). These electrons generate double-strand breaks in DNA through internalization of radiopharmaceuticals into the cell nucleus and kill neighboring tumor cells *via* a bystander effect (27-29). The formulation of indium-111-labeled PEGylated liposomes has been used successfully to characterize prolonged retention in tumor-targeted radiotherapy. Therefore, prior to a preclinical therapeutic trial, the goal of this study was to investigate the difference of pharmacokinetics and biodistribution, effectiveness of passive targeting and tumor growth inhibition between 0.9 mol% and 6 mol% PEGylated liposomes encapsulated with indium-111 in human colorectal carcinoma (HT-29/*luc*) xenografted mice. Since our previous use of 0.9 mol% PEGylated liposomes caused the highest amount of radioactivity in the RES (44), this study was to investigate the reduction in uptake of radioactivity by the RES using 6 mol% rather than 0.9 mol% PEGylated liposomes. The results could provide useful information for using PEGylated liposomes encapsulated with indium-111 and an anticancer drug, such as vinorelbine (VNB), in a human tumor-bearing animal model.

Materials and Methods

Cell culture. The human colorectal carcinoma cell line (HT-29) was purchased from the Bioresource Collection and Research Center, Hsinchu, Taiwan, R.O.C. This cell line was transfected with the luciferase gene (*luc*) as reporter. HT-29/*luc* tumor cells were maintained in RPMI-1640 medium with 10% heat-inactivated fetal bovine serum (FBS) (Hyclone, Utah, USA) and supplemented with L-glutamine, sodium bicarbonate, 100 units/ml penicillin and 100 μg/ml streptomycin. The stably transfected HT-29/*luc* cells were grown at 37˚C in a humidified atmosphere containing 5% CO_2 and contained 500 μg/ml G418 (Merck, USA) to maintain stable expression of the *luc* gene (8).

Tumor cell preparation. HT-29/*luc* tumor cells were harvested by brief incubation with trypsin at 37˚C and a single-cell suspension was prepared in RPMI-1640 (FBS-free) medium. Male NOD/SCID mice were inoculated with 2×10^6/200 μl tumor cells subcutaneously in the dorsal region of the right thigh.

Preparation of liposomes. The preparation of PEGylated liposomes were carried out as previousely described by Tseng *et al*. (30). Small unilamellar vesicles (SUV, ~100 nm diameter) were prepared by a combination of the standard thin-film hydration method and repeated extrusion. PEG-distearoylphosphatidylethanolamine (DSPE) of 0.9 and 6 mol% was prepared using the following ratios: disteroyl-phosphatidylcholine (DSPC):cholesterol (Chol):DSPE covalently linked polyethylene glycol (PEG) of 2:1:0.027 for 0.9 mol% PEG-DSPE or 2:1:0.18 for 6 mol% PEG-DSPE. The above mixtures were dissolved in chloroform and placed in a round-bottomed flask. The solvent was removed by rotary evaporation under reduced pressure. The resulting dry lipid film was hydrated at 60˚C in an aqueous solution of triethylammonium sucrose octasulfate (TEA-SOS; 0.6 M triethylammonium, pH 5.7-6.2) and dispersed by hand shaking at 60˚C. The suspension was frozen and thawed 5 times followed by repeated extrusion through polycarbonate membrane filters (Costar, Cambridge, MA, USA) of 0.1 mm pore size 3 times and 0.05 mm 7 times using high pressure extrusion equipment (Lipex Biomembranes, Vancouver, BC, USA) at 60˚C. After extrusion, the extra-liposomal salt was removed by a Sephadex G-50 column eluted with histidine-sucrose buffer (24 mM histidine hydrogen chloride, 90 g/l sucrose, pH adjusted to 6.0 with NaOH) (8).

Radiolabeling of ^{111}In-oxine. Fifteen microliters of 68 mM 8-hydroxyquinoline (oxine; Sigma-Aldrich Co., St. Louis, MO, USA) in ethanol were added to 10 μl of ^{111}In (indium chloride in 0.05 M HCl; 0.01-1 mCi; Perkin Elmer, Boston, MA, USA) in 400 μl of 0.1 M sodium acetate buffer (pH 5.5) and then incubated at 50˚C for 20 min. The lipophilic components were extracted 3 times with 0.5 ml of chloroform and then dried using a rotary evaporator. The labeling efficiency with ^{111}In-oxine was determined by an instant thin layer chromatography (ITLC) method. ITLC was performed on a silica gel-impregnated glass fiber sheet (ITLCTM SG; Pall Corporation, New York, NY, USA) using ethanol as the developing agent. In this system, free ^{111}In-Cl_3 remains at the origin (Rf=0) while ^{111}In-oxine moves to the top of the strip (Rf=0.9-1.0). The radiochemical yield was generally greater than 90% ^{111}In-oxine (8).

Preparation of ^{111}In liposomes. The extracted ^{111}In-oxine in chloroform was evaporated to dryness. This was followed by the addition of 20 μl of ethanol and 80 μl of distilled water into the vial, and then the mixture was incubated with 1.5 ml of liposomes for 30 min at 37˚C. Two milligrams of EDTA were added to chelate any residual free indium-111 and to promote prompt excretion after *i.v.* injection. Liposomes were labeled by incubating with 2 mCi ^{111}In-

oxine for 30 min at room temperature. The entrapment of indium-111 within liposomes (6 mol% PEG) was assayed by loading a 100 μl sample onto a Sephadex™ G-50 Fine (40×8 mm) column, and eluted with normal saline. Eight consecutive 0.5 ml fractions were collected; the liposomes were eluted from the second and the third fractions. The radioactivity of each fraction was measured using either a dose calibrator (CRC-15R; Capintec; Bioscan, Washington DC, USA) or a gamma scintillation counter (Cobra II Autogamma; Packard, Downers Grove, IL, USA). The entrapment of indium-111 was more than 90% (8).

Pharmacokinetics and biodistribution of ^{111}In liposomes in the HT-29/luc tumor-bearing mice. Pharmacokinetics and biodistribution studies were performed when tumor size reached 70±10 mm^3. At this time, the tumor-bearing NOD/SCID mice were randomly divided into two groups and one group received intravenous administration of 70 μCi (2.59 MBq)/100 μl of ^{111}In-labeled 0.9 mol% and 6 mol% PEGylated liposomes, respectively. In pharmacokinetic studies (n=6 for each group), blood samples (1 μl) were collected from mouse tail veins at various time points (1, 5, 15 and 30 min, and 1, 2, 4, 8, 12, 16, 20, 24, 28, 32, 36, 40, 44, 48, 56, 64 and 72 h) after drug administration. The radioactivity of blood samples was measured using a gamma scintillation counter (Cobra II Auto-Gamma counter; Packard). Data were expressed as the percentage of the injected dose per milliliter (% ID/ml). Pharmacokinetic parameters were analyzed using WinNonlin software version 5.0.1 (Pharsight Corp., Mountain View, CA, USA). Noncompartmental analysis (NCA) model 201 (IV-Bolus Input) of plasma data was used with the log/linear trapezoidal rule. Parameters, including terminal half-life ($T_{1/2}\lambda z$), C_{max}, total body clearance (Cl) and area under the curve (AUC) were determined. In biodistribution studies (n=4 for each group), mice were sacrificed at 1, 4, 24, 48 and 72 h post injection. Anatomization was carried out and the tissues/organs of interest including blood, heart, lung, liver, stomach, spleen, pancreas, large and small intestines, bladder, urine, kidneys, muscle, bone marrow and the tumor were excised and collected. The net tissue weights were obtained and radioactivity was measured using the same counter. The uptake of ^{111}In-labeled PEGylated liposomes in various tissues/organs was expressed as counts per minute (cpm) with decay correction standards and was normalized as % ID per gram (% ID/g) according to the following formula:

$$\%\ ID/g=(A_0 \times 1000)/[\text{Injected dose } (\mu Ci) \times 3.7 \times 10^4 \times 60 \times Eff \times \text{tissue/organ weight}]$$

where $\ln (A_1/A_0)=-0.693t/t_{1/2}$, in which A_1 is the radioactivity (cpm) of tissue assayed with the gamma counter, A_0 is the decay-corrected radioactivity (cpm) of tissue, Eff is the counting efficiency of the gamma scintillation counter (Eff=0.42), $t_{1/2}$=half-life of radioisotope, *t* is time post injection, and the organ weight is in mg (31).

2D Planar gamma scintigraphy. Based on the biodistribution results, mice were anesthetized with isoflurane (Abbott Laboratories, Queenborough, Kent, UK) using a vaporizer system (A.M. Bickford, Wales Center, NY, USA); then 2D planar gamma scintigraphy was performed on the HT-29/*luc* tumor-bearing mice at 4, 24, 48 and 72 h post injection with 70 μCi (2.59 MBq)/100 μl of 0.9 mol% and 6 mol% PEG ^{111}In liposomes, respectively. A dual head gamma camera (E.Cam Multiangle Cardiac; Siemens, Münich, Germany) equipped with a 4 mm pinhole collimator and ICON P computer system (Siemens) was used for the gamma imaging. The anesthetized mice were placed prone on the camera's pinhole collimator and the images were acquired as a 256×256 matrix for 20 min. Regions of interest (ROIs) of the tumor, liver, spleen and muscle areas were drawn and analyzed (8).

Bioluminescence imaging (BLI). In vivo BLI was carried out on the HT-29/*luc* tumor-bearing NOD/SCID mice using a cooled IVIS50® animal imaging system (Xenogen, Corp., Alameda, CA, USA). The IVIS50® system consists of a cooled CCD camera mounted in a light-tight specimen chamber, a cryogenic refrigeration unit, a camera controller and a computer system for data analysis. This system provides high signal-to-noise images of the luciferase signals emitted from within living animals. D-Luciferin is a chemical substrate of the firefly luciferase that creates the bioluminescence photon flux in the presence of oxygen and ATP. The photons emitted from the target site penetrate across the mammalian tissues and could be externally detected and quantified using a sensitive light-imaging system (31). Based on this property, the mice were anesthetized with 1-3% isoflurane using a vaporizer system and intraperitoneally injected (*i.p.*) with 150 mg/kg D-Luciferin 15 min prior to imaging. Image acquisition time was 5 s dependent on the bioluminescent intensity of the tumors. The photon flux emitted from the ROIs of tumor sites were detected by the IVIS50® imaging system and the displayed images of the tumor sites were drawn around and quantified in photons/s (ph/s) using Living Image software (Xenogen, Corp.) (8).

Tumor growth tracing. A total of 2×10^6 HT-29/*luc* tumor cells were subcutaneously implanted into the dorsal region of the right thigh of male NOD/SCID mice (n=8). Tumor growth curves *in vivo* were established using a digital caliper when the bulge was visible. Tumor volume was calculated as the following: 0.523 × (length × width × thickness).

Statistical analysis. Student's *t*-test for significant difference between control and drug-treated mice, or between 0.9 mol% and 6 mol% PEGylated liposomal drugs was performed. The significance was defined as $p<0.05$ (marked as *) and $p<0.01$ (marked as **).

Results

Pharmacokinetics of 0.9 mol% and 6 mol% PEG ^{111}In liposomes in HT-29/luc tumor-bearing mice. The radioactivity in the blood of the HT-29/*luc* tumor-bearing mice was collected and calculated after intravenous (*i.v.*) administration of 0.9 mol% and 6 mol% PEG ^{111}In liposomes, respectively. The concentration of radioactivity represented as % ID/ml is shown in Figure 1. The parameters obtained from the pharmacokinetic study are summarized in Table I. The terminal half-life ($T_{1/2}\lambda z$) of 6 mol% and 0.9 mol% PEG ^{111}In liposomes was 16.2 h and 18.3 h, respectively. The maximum concentration of radioactivity (C_{max}) in the blood was calculated as being from 49.37 to 50.84% ID/ml at 0.02 h by both treatments. The total body clearance of radioactivity in the 0.9 mol% PEG ^{111}In liposomes group was 0.27 ml/h, and was 0.16 ml/h for the 6 mol% PEG ^{111}In liposomes group. The $AUC_{(o\rightarrow\infty)}$ of 6 mol% PEGylated liposomes was also higher than that of 0.9 mol% PEGylated liposomes.

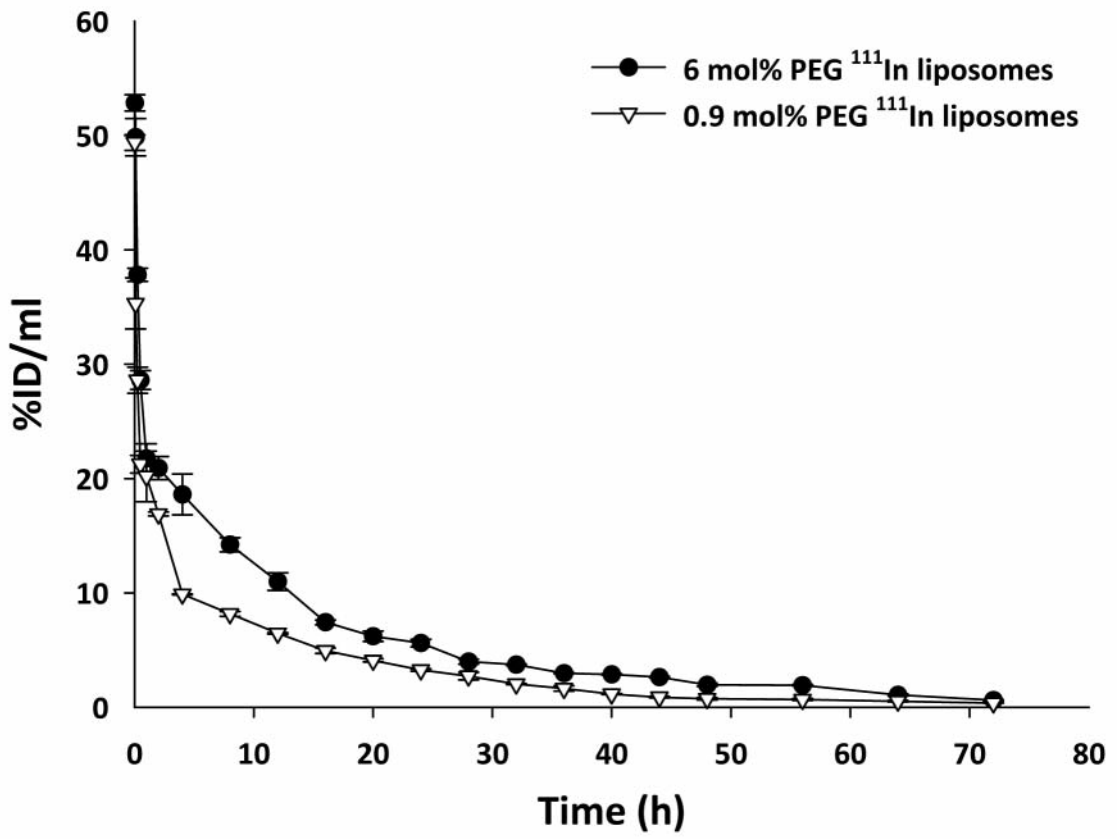

Figure 1. *Pharmacokinetics of 0.9 mol% and 6 mol% PEG ^{111}In liposomes in NOD/SCID mice bearing HT-29/luc tumors. Radioactivity- time curves of both treatments were calculated from the blood samples after i.v. administration. Data are represented as %ID/ml for each time point (mean±SE, n=6). The experiments were repeated three times.*

Biodistribution of 0.9 mol% and 6 mol% PEG ^{111}In liposomes in HT-29/luc tumor-bearing mice. The accumulation of liposomal drugs in the tissues of the HT-29/*luc* tumor-bearing NOD/SCID mice (n=4) were measured at different time points after 70 μCi (2.59 MBq)/100 μl administration of 0.9 mol% and 6 mol% PEG ^{111}In liposomes. The concentration of radioactivity in the blood decreased rapidly from 19.76±1.28% ID/g to 0.61±0.06% ID/g and from 20.19±2.21% ID/g to 0.29±0.04% ID/g after treatment with 6 mol% and 0.9 mol% PEG ^{111}In liposomes, respectively (Table II and III). A rapid clearance of radioactivity from the blood at 24 h post injection was found. Prominent radioactivity accumulation was found in the liver, spleen and kidneys in all treatments, with maximum levels of 14.65±1.54 *vs*. 37.61±2.06, 25.27±3.22 *vs*. 164.16±16.35, and 23.72±2.76 *vs*. 28.36±3.72% ID/g, for 6 mol% *vs*. 0.9 mol% PEG ^{111}In liposomes treatments. On the contrary, the maximum uptake of the tumor (70±10 mm^3) was 15.48±2.21 *vs*. 8.93±1.76% ID/g at 48 h post-treatment. The AUCs of 6 mol% PEG ^{111}In liposomes revealed a prolonged circulation of the drug in the plasma, with a significant decrease in the liver, spleen, small intestine and kidneys as well as bone marrow, and enhanced accumulation in the tumor, suggesting the EPR effect in the tumor was strengthened when PEG was increased from 0.9 mol% to 6 mol% (Table IV).

Table I. *Pharmacokinetic parameter estimates of HT-29/luc human colorectal carcinoma xenografted NOD/SCID mice (n=6) after 0.9 mol% and 6 mol% PEG ^{111}In liposomes (i.v.) administration.*

Parameter	Unit	6 mol% PEG ^{111}In liposomes	0.9 mol% PEG ^{111}In liposomes
$T_{1/2}\lambda z$	h	16.21	18.31
C_{max}	% ID/ml	50.84	49.37
Cl	ml/h	0.16	0.27
$AUC_{(o\rightarrow\infty)}$	h×% ID/ml	444.35	257.39

Parameters were calculated with WinNonlin program for a noncompartmental model. $T_{1/2}\lambda z$, Half-life; C_{max}, maximum concentration; Cl, clearance; $AUC_{(o\rightarrow\infty)}$, area under the curve.

Table II. *Biodistribution of HT-29/luc tumor-bearing NOD/SCID mice after 6 mol% PEG ^{111}In liposomes (i.v.) administration.*

	Time after administration (h)				
Organ	1	4	24	48	72
Blood	19.76±1.28	18.61±1.78	5.61±0.33	1.96±0.14	0.61±0.06
Heart	4.39±0.21	4.02±0.13	1.72±0.03	1.57±0.05	0.61±0.03
Lung	7.61±0.37	12.88±1.43	5.98±0.71	3.37±0.41	4.03±0.77
Liver	4.94±0.60	7.44±1.29	9.91±1.04	12.39±1.15	14.65±1.54
Stomach	4.15±0.17	2.98±0.50	2.60±0.18	2.50±0.19	2.30±0.09
Spleen	7.34±1.08	13.82±2.36	17.58±2.52	25.27±3.22	23.92±3.48
Pancreas	3.01±0.16	2.71±0.18	1.79±0.14	1.41±0.11	1.40±0.13
Large intestine	2.80±0.19	3.12±0.29	2.74±0.29	2.57±0.46	2.06±0.06
Small intestine	5.31±0.54	6.27±0.37	4.33±0.27	4.49±0.38	3.17±0.38
Bladder	4.17±0.19	2.34±0.25	2.01±0.19	1.91±0.11	1.46±0.12
Urine	2.84±0.24	2.11±0.16	1.69±0.10	1.19±0.09	0.85±0.12
Kidneys	18.32±2.96	23.72±2.76	16.52±1.56	12.38±1.86	8.22±1.80
Muscle	1.50±0.03	1.13±0.14	0.80±0.12	0.66±0.10	0.45±0.12
Bone marrow	5.05±0.42	5.77±0.68	4.12±0.36	4.39±0.30	4.21±0.28
Tumor	2.91±0.29	4.10±1.74	8.22±0.90	15.48±2.21	10.28±0.48
Tumor/blood	0.15	0.22	1.47	7.90	16.85
Tumor/muscle	1.94	3.63	10.28	23.45	22.84

Values are expressed as % ID/g, mean±SE (n=4 at each time point).

Table III. *Biodistribution of HT-29/luc tumor-bearing NOD/SCID mice after 0.9 mol% PEG ^{111}In liposomes (i.v.) administration.*

	Time after administration (h)				
Organ	1	4	24	48	72
Blood	20.19±2.21	13.08±1.81	3.97±0.62	1.62±0.19	0.29±0.04
Heart	3.27±0.17	2.56±0.31	1.58±0.08	1.39±0.07	0.52±0.04
Lung	7.61±0.37	12.88±1.43	5.98±0.71	3.37±0.41	4.03±0.77
Liver	12.55±1.49	19.86±1.81	27.83±3.63	33.10±4.17	37.61±2.06
Stomach	4.11±0.74	3.03±0.26	2.86±0.39	2.55±0.18	2.10±0.19
Spleen	27.22±3.22	36.86±3.36	94.14±11.06	134.19±17.92	164.16±16.35
Pancreas	3.12±0.37	3.02±0.30	1.85±0.11	1.79±0.12	1.73±0.18
Large intestine	3.66±0.45	2.53±0.19	2.51±0.21	2.16±0.46	2.26±0.06
Small intestine	9.26±0.71	7.53±0.62	6.80±0.57	5.90±0.74	6.06±0.66
Bladder	3.71±0.32	3.12±0.12	2.52±0.27	2.10±0.19	1.78±0.17
Urine	3.12±0.37	3.55±0.31	1.75±0.10	1.24±0.19	0.33±0.05
Kidneys	14.89±1.51	28.36±3.72	24.59±2.66	19.99±2.03	15.00±1.97
Muscle	1.50±0.18	1.75±0.14	1.07±0.09	0.72±0.09	0.55±0.04
Bone marrow	5.16±0.40	8.04±0.68	7.06±0.53	6.88±0.55	6.43±0.34
Tumor	2.23±0.20	3.19±0.23	4.65±0.68	8.93±1.76	5.94±0.63
Tumor/blood	0.11	0.24	1.17	5.51	20.48
Tumor/muscle	1.49	1.82	4.35	12.40	10.80

Values are expressed as % ID/g, mean±SE (n=4 at each time point).

Gamma scintigraphy of xenografted mice. 2D Planar gamma scintigraphy of the HT-29/*luc* tumor-bearing NOD/SCID mice was performed at various time points post *i.v.* injection with 70 μCi (2.59 MBq)/100 μl of 0.9 mol% and 6 mol% PEG ^{111}In liposomes. The values of gamma photon counts and tumor/muscle (T/M) ratios (Table V) from gamma scintigraphy were well correlated to that of the biodistribution, with the highest uptake at 48 h by 6 mol% PEG ^{111}In liposomes treatment.

Tumor growth inhibition. Male NOD/SCID mice were transplanted with 2×10^6 HT-29/*luc* tumor cells in the subcutaneous dorsal region of the right thighs. Tumor growth monitoring was initiated on day 16 after tumor cell

Table IV. *Areas under the curve (AUC) and RR-AUCs for 6 mol% vs. 0.9 mol% PEG ^{111}In liposomes after i.v. administration in HT-29/luc tumor-bearing NOD/SCID mice.*

Organ/group	AUC		RR-AUC (6 mol% *vs.* 0.9 mol% PEG ^{111}In liposomes)
	6 mol% PEG ^{111}In liposomes	0.9 mol% PEG ^{111}In liposomes	
Blood	421.38	247.48	1.70**
Heart	139.84	111.97	1.25
Lung	427.71	544.78	0.79
Liver	789.12	2117.76	0.37**
Stomach	189.54	194.44	0.97
Spleen	1457.54	7753.78	0.19**
Pancreas	128.71	146.77	0.88
Large intestine	189.67	172.36	1.10
Small intestine	326.46	473.90	0.69*
Bladder	142.50	172.37	0.83
Urine	107.19	121.00	0.89
Kidney	1077.66	1564.01	0.69*
Muscle	55.48	70.07	0.79
Bone marrow	325.34	502.97	0.65*
Tumor	730.15	430.16	1.70**

*$p<0.05$, **$p<0.01$, significant difference between 0.9 mol% and 6 mol% PEG ^{111}In liposomes.

Table V. *Gamma photon counts of tumor, tumor/muscle (T/M) ratios, tumor/liver (T/L) ratios, and tumor/spleen (T/S) ratios were obtained from gamma scintigraphy after i.v. injection of 0.9 mol% and 6 mol% PEG ^{111}In liposomes in HT-29/luc tumor-bearing SCID mice (n=5).*

Time (hours)	6 mol% PEG ^{111}In liposomes				0.9 mol% PEG ^{111}In liposomes			
	γ Count	T/M	T/L	T/S	γ Count	T/M	T/L	T/S
4	4835.60±157.20	1.63	0.12	0.10	4436.00±168.20	1.67	0.09	0.04
24	6446.80±162.82	2.09	0.15	0.13	5051.40±176.30	1.72	0.06	0.02
48	10388.60±256.83	3.55	0.23	0.18	6855.60±159.72	2.35	0.07	0.02
72	8802.00±234.30	3.01	0.18	0.15	6046.20±239.25	2.02	0.05	0.01

Table VI. *Tumor growth inhibition of HT-29/luc tumor xenografted NOD/SCID mice (n=8) after i.v. administration of drugs. Tumors were measured twice per week using a digital caliper. The data were calculated from the time point when tumor size reached 6-fold that of the initial tumor volume (i.e. 50 mm^3).*

Treatment	Tumor growth time (days)	Tumor growth delay (days)	Mean growth inhibition rate	*P*-value
6 mol% PEG ^{111}In liposomes	45.85	10.63	0.49	<0.01
0.9 mol% PEG ^{111}In liposomes	38.53	3.31	0.73	<0.01
Vehicle (control)	35.22	-	-	-

Tumor growth time (TGT): The time needed to reach 6-fold that of the initial tumor volume. Tumor growth delay (TGD): The tumor growth time of the treated group–that of the control group. Mean growth inhibition rate (IR): Growth rate of treated group/growth rate of the control group. The values of IR were calculated on the 55th day of treatment.

inoculation (tumor size~50±5 mm^3). Multiple doses of 0.9 mol% and 6 mol% PEG ^{111}In liposomes [70 μCi (2.59 MBq)/100 μl] were *i.v.* administrered once a week for one month. Both BLI and caliper measurements were performed twice a week (Figure 2A and 3). The tumor growth delay time was 10.63 days and the greater inhibition rate of tumor growth was 0.49 by 6 mol% PEG ^{111}In liposomes treatment ($p<0.01$) (Table VI). The photon counts of luminescence (Figure 2B) were collected and measured from the ROIs of tumor sites (n=4). A significant inhibition of tumor growth

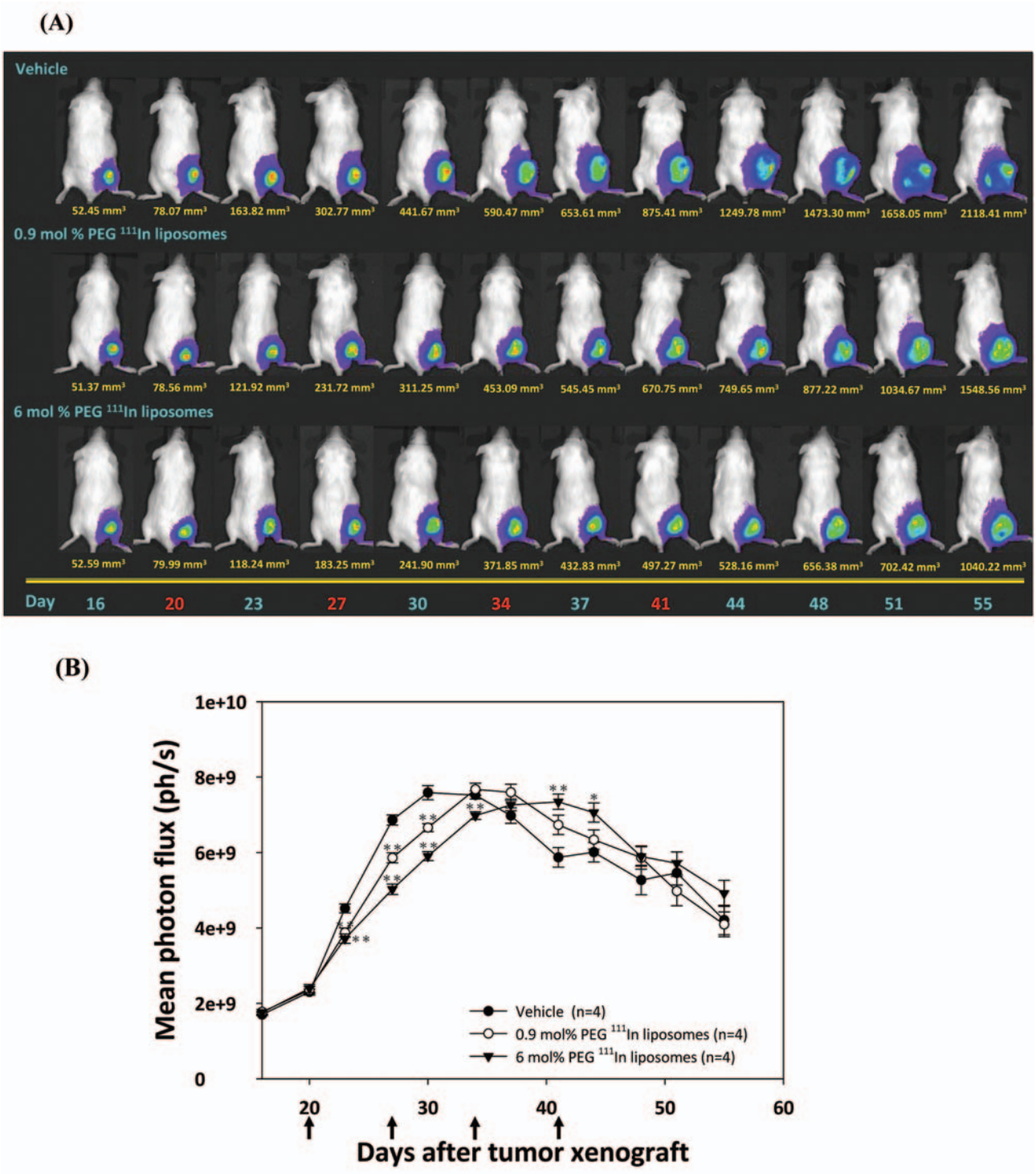

Figure 2. *A, In vivo bioluminescence imaging (BLI) of HT-29/luc tumor-bearing NOD/SCID mice. HT-29/luc tumor cells were transplanted subcutaneously into the dorsal region of the right thigh of mice. At 20 days of inoculation (tumor size~ 70±10 mm^3) and afterwards, the mice were i.v. administrered liposomes with 0.9 mol% or 6 mol% PEG ^{111}In liposomes, respectively, at indicated time points (as shown by red figures). B, The BLI photon flux distribution of the tumors of mice treated with 0.9 mol% or 6 mol% PEG ^{111}In liposomes. The 6 mol% PEG ^{111}In liposomes group showed a significantly lower level of photon counts before the 35th day of inoculation. A lower level of photon counts corresponds to tumor growth inhibition. Data are expressed as mean±SE. *p<0.05, **p<0.01, significantly different from control by Student's t-test. Black arrows indicate the time of injection. The experiments were repeated three times.*

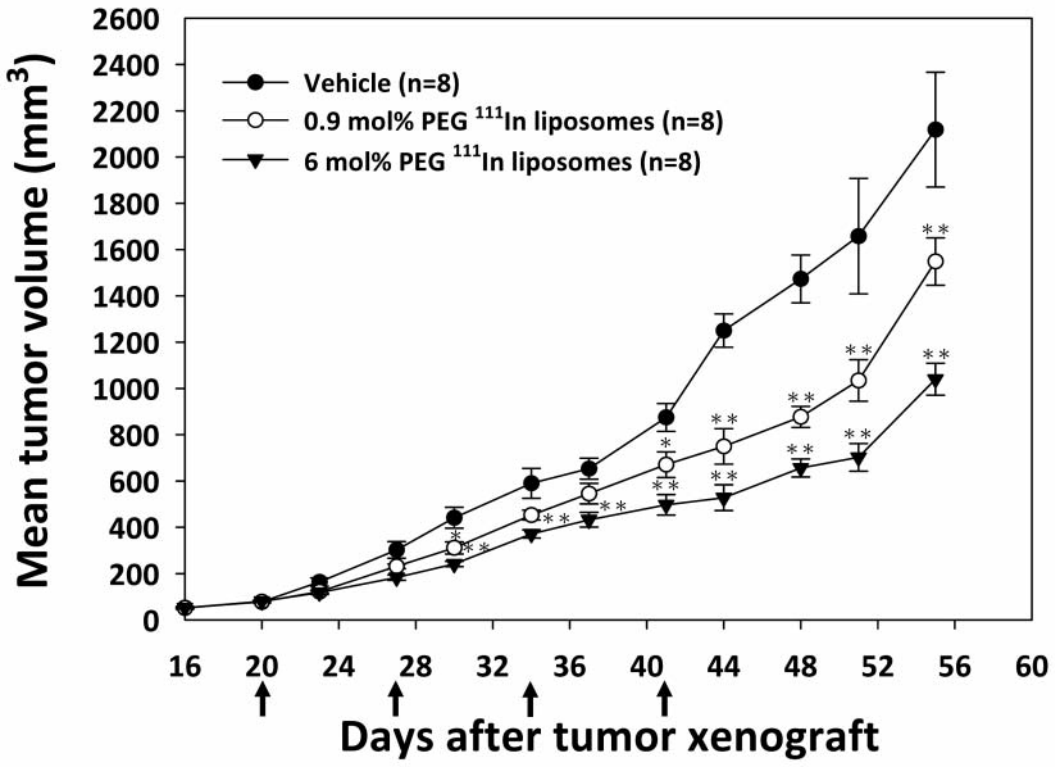

Figure 3. *The tumor growth curves of HT-29/luc tumor xenografts. Tumor cells were transplanted subcutaneously into the dorsal region of the right thigh of male NOD/SCID mice and the tumor assayed with a digital caliper. The greatest tumor growth inhibition was found with treatment with 6 mol% PEG ^{111}In liposomes. Data are expressed as mean±SE. *p<0.05, **p<0.01, Student's t-test. Black arrows indicate the time of injection. The experiments were repeated three times.*

was found by 6 mol% PEG ^{111}In liposomes treatment, which corresponds with lower tendency of photon flux distribution. No significant difference was observed during days 44 to 55. This may have been caused by the characteristics of the tumor cell line or the induction of tumor necrosis as the tumor size reaches more than 500 mm^3.

Discussion

Liposomal carriers modified with PEG has been used as a vehicle for therapeutic agent delivery, such as of doxorubicin and daunorubicin, and are in various stages of preclinical and clinical development (16-22). However, the degree of PEGylation may also influence the stability of nanoparticles. Excessive PEGylation would disturb the balance of hydrophilicity and hydrophobicity by disrupting the integrity of the surface lipid bilayer (32). On the other hand, a lower concentration of PEGylation would increase the RES uptake and renal elimination (31). Therefore, an optimal level of PEGylation is important for ideal liposomal nanoparticles as shown by Li and Huang with 5 mol% PEGylated liposomes (32). In this study, we also obtained better spatial and temporal distribution of ^{111}In-labeled PEGylated liposomes using 6 mol% PEG significantly prolonging the drug circulation in the plasma, attenuating the injected dose (% ID/g) in the liver, spleen, kidneys, small intestine and bone marrow (p<0.05), while enhancing the accumulation in the tumor. The total body clearance of radioactivity was 1.7-fold lower and the AUC 1.7-fold higher in 6 mol% PEG ^{111}In liposomes than in those of 0.9 mol% PEG (Table I). In mice treated with 6 mol% PEG ^{111}In liposomes, the average amount of radioactivity in the liver and spleen was lower by 2.68- and 5.32-fold, respectively, over a 72 h period as compared to that in mice treated with 0.9 mol% PEG ^{111}In liposomes (Table IV). The uptake in the small intestine, kidneys and the bone marrow decreased by 1.45-, 1.45- and 1.55-fold, respectively. These results suggested that PEGylation indeed affected the accumulation and distribution of liposomal drug. The tumor uptake with 6 mol% PEG ^{111}In liposomes was also better. In both groups, the tumor uptake gradually increased with time, with maximum accumulation at 48 h post treatment (Tables II and III). Non-invasive and dynamic molecular imaging using animal positron-emission tomography (microPET), magnetic resonance imaging (microMRI), BLI, and single photon-emission computed tomography (SPECT) is often applied for efficacy evaluation in diagnosis and therapeutics, new drug

discovery and preclinical studies (33-35). Molecular imaging also provides a faster and convenient approach for tumor growth and metastatic tracing, targeting efficiency and therapeutic response during the treatment course (36, 37). Since the animal model used in this study carried a luciferase reporter gene, both BLI and digital caliper assays were used to evaluate the diagnostic and therapeutic efficiency. Again, 6 mol% PEG ^{111}In liposomes showed a better inhibition rate ($p<0.01$) than that of 0.9 mol% with these two approaches (Figures 2 and 3).

Using radiolabeled liposomal drugs as therapeutic agents, the absorbed radiation doses in critical organs should be considered for future application in clinical trials. An understanding of the distribution in these organs, such as the liver, spleen, kidneys and bone marrow, is crucial for the understanding normal tissue tolerance, such as myelotoxicity and secondary organ toxicities. Lower critical tissue toxicity may be achieved by various strategies including suitable PEGylation (5-10 mol% PEG) of the liposomal surface (13, 38), optimal particle size (~100 nm diameter) (39), neutral lipid structure (±10 mV for potential) (40, 41); receptor-mediating immunoliposome, pH-sensitive liposome (42), thermal-sensitive liposome (43), and prior administration of empty liposomes to occupy the RES-rich organs may also be considered to improve the bioavailability of nanomedicine.

Conclusion

Liposomes with 6 mol% PEG (100 nm in diameter and 5.06 mV for ζ potential) were shown to have higher tumor uptake but lower toxicity in organs such as the liver, spleen, kidneys, small intestine as well as bone marrow than those with 0.9 mol% PEG in mice with HT-29/*luc* human colorectal adenocarcinoma xenograft. Liposomes modified with 6 mol% PEG, instead of 0.9 mol% , showed longer drug circulation in the plasma, enhanced tumor targeting and improved the therapeutic efficiency.

Acknowledgements

This study was supported by grant 95A1-NMPPO1-007 from the National Health Research Institute, Taipei, Taiwan, R.O.C. The nanoliposomes were kindly provided by Taiwan Liposome Company, Taipei, Taiwan, R.O.C. The authors also appreciated the support from the MAGIC core of the National Research Program for Genomic Medicine, National Science Council, Taipei, Taiwan, R.O.C.

References

1 Gregoriadis G: The carrier potential of liposomes in biology and medicine (first of two parts). N Engl J Med *295*: 704-710, 1976.

2 Beaumier PL and Hwang KJ: An efficient method for loading indium-111 into liposomes using acetylacetone. J Nucl Med *23*: 810-815, 1982.

3 McDougall IR, Dunnick JK, Goris ML and Kriss JP: *In vivo* distribution of vesicles loaded with radiopharmaceuticals: a study of different routes of administration. J Nucl Med *16*: 488-491, 1975.

4 Caride VJ, Taylor W, Cramer JA and Gottschalk A: Evaluation of liposome-entrapped radioactive tracers as scanning agents. Part 1: Organ distribution of liposome (^{99m}Tc-DTPA) in mice. J Nucl Med *17*: 1067-1072, 1976.

5 Espinola LG, Beaucaire J, Gottschalk A and Caride VJ: Radiolabeled liposomes as metabolic and scanning tracers in mice. II. In-111 oxine compared with Tc-99m DTPA, entrapped in multilamellar lipid vesicles. J Nucl Med *20*: 434-440, 1979.

6 Allen TM and Cullis PR: Drug delivery systems: entering the mainstream. Science *303*: 1818-1822, 2004.

7 Torchilin VP: Recent advances with liposomes as pharmaceutical carriers. Nat Rev Drug Discov *4*: 145-160, 2005.

8 Chow TH, Lin YY, Hwang JJ, Wang HE, Tseng YL, Pang VF, Wang SJ, Whang-Peng J and Ting G: Diagnostic and therapeutic evaluation of ^{111}In-vinorelbine-liposomes in a human colorectal carcinoma HT-29/luc-bearing animal model. Nucl Med Biol *35*: 623-634, 2008.

9 Bakker-Woudenberg IA, Lokerse AF and Roerdink FH: Antibacterial activity of liposome-entrapped ampicillin *in vitro* and *in vivo* in relation to the lipid composition. J Pharmacol Exp Ther *251*: 321-327, 1989.

10 Nacucchio MC, Gatto Bellora MJ, Sordelli DO and D'Aquino M: Enhanced liposome-mediated antibacterial activity of piperacillin and gentamicin against gram-negative bacilli *in vitro*. J Microencapsul *5*: 303-309, 1988.

11 Messerer CL, Ramsay EC, Waterhouse D, Ng R, Simms EM, Harasym N, Tardi P, Mayer LD and Bally MB: Liposomal irinotecan: formulation development and therapeutic assessment in murine xenograft models of colorectal cancer. Clin Cancer Res *10*: 6638-6649, 2004.

12 Boerman OC, Storm G, Oyen WJ, van Bloois L, van der Meer JW, Claessens RA, Crommelin DJ and Corstens FH: Sterically stabilized liposomes labeled with indium-111 to image focal infection. J Nucl Med *36*: 1639-1644, 1995.

13 Woodle MC and Lasic DD: Sterically stabilized liposomes. Biochim Biophys Acta *1113*: 171-199, 1992.

14 Huang SK, Lee KD, Hong K, Friend DS and Papahadjopoulos D: Microscopic localization of sterically stabilized liposomes in colon carcinoma-bearing mice. Cancer Res *52*: 5135-5143, 1992.

15 Huang SK, Martin FJ, Jay G, Vogel J, Papahadjopoulos D and Friend DS: Extravasation and transcytosis of liposomes in Kaposi's sarcoma-like dermal lesions of transgenic mice bearing the HIV *tat* gene. Am J Pathol *143*: 10-14, 1993.

16 Northfelt DW, Dezube BJ, Thommes JA, Miller BJ, Fischl MA, Friedman-Kien A, Kaplan LD, Du Mond C, Mamelok RD and Henry DH: Pegylated-liposomal doxorubicin *versus* doxorubicin, bleomycin, and vincristine in the treatment of AIDS-related Kaposi's sarcoma: results of a randomized phase III clinical trial. J Clin Oncol *16*: 2445-2451, 1998.

17 Gordon AN, Fleagle JT, Guthrie D, Parkin DE, Gore ME and Lacave AJ: Recurrent epithelial ovarian carcinoma: a randomized phase III study of pegylated liposomal doxorubicin *versus* topotecan. J Clin Oncol *19*: 3312-3322, 2001.

18 Harris L, Batist G, Belt R, Rovira D, Navari R, Azarnia N, Welles L and Winer E: Liposome-encapsulated doxorubicin compared with conventional doxorubicin in a randomized multicenter trial as first-line therapy of metastatic breast carcinoma. Cancer *94*: 25-36, 2002.

19 Batist G, Ramakrishnan G, Rao CS, Chandrasekharan A, Gutheil J, Guthrie T, Shah P, Khojasteh A, Nair MK, Hoelzer K, Tkaczuk K, Park YC and Lee LW: Reduced cardiotoxicity and preserved antitumor efficacy of liposome-encapsulated doxorubicin and cyclophosphamide compared with conventional doxorubicin and cyclophosphamide in a randomized, multicenter trial of metastatic breast cancer. J Clin Oncol *19*: 1444-1454, 2001.

20 Gill PS, Wernz J, Scadden DT, Cohen P, Mukwaya GM, von Roenn JH, Jacobs M, Kempin S, Silverberg I, Gonzales G, Rarick MU, Myers AM, Shepherd F, Sawka C, Pike MC and Ross ME: Randomized phase III trial of liposomal daunorubicin *versus* doxorubicin, bleomycin, and vincristine in AIDS-related Kaposi's sarcoma. J Clin Oncol *14*: 2353-2364, 1996.

21 Rosenthal E, Poizot-Martin I, Saint-Marc T, Spano JP and Cacoub P: Phase IV study of liposomal daunorubicin (DaunoXome) in AIDS-related Kaposi sarcoma. Am J Clin Oncol *25*: 57-59, 2002.

22 Stewart S, Jablonowski H, Goebel FD, Arasteh K, Spittle M, Rios A, Aboulafia D, Galleshaw J and Dezube BJ: Randomized comparative trial of pegylated liposomal doxorubicin *versus* bleomycin and vincristine in the treatment of AIDS-related Kaposi's sarcoma. International Pegylated Liposomal Doxorubicin Study Group. J Clin Oncol *16*: 683-691, 1998.

23 Muggia FM, Hainsworth JD, Jeffers S, Miller P, Groshen S, Tan M, Roman L, Uziely B, Muderspach L, Garcia A, Burnett A, Greco FA, Morrow CP, Paradiso LJ and Liang LJ: Phase II study of liposomal doxorubicin in refractory ovarian cancer: antitumor activity and toxicity modification by liposomal encapsulation. J Clin Oncol *15*: 987-993, 1997.

24 Ranson MR, Carmichael J, O'Byrne K, Stewart S, Smith D and Howell A: Treatment of advanced breast cancer with sterically stabilized liposomal doxorubicin: results of a multicenter phase II trial. J Clin Oncol *15*: 3185-3191, 1997.

25 Gabizon A, Shmeeda H and Barenholz Y: Pharmacokinetics of pegylated liposomal Doxorubicin: review of animal and human studies. Clin Pharmacokinet *42*: 419-436, 2003.

26 Papahadjopoulos D, Allen TM, Gabizon A, Mayhew E, Matthay K, Huang SK, Lee KD, Woodle MC, Lasic DD, Redemann C and Martin FJ: Sterically stabilized liposomes: improvements in pharmacokinetics and antitumor therapeutic efficacy. Proc Natl Acad Sci USA *88*: 11460-11464, 1991.

27 Howell RW, Narra VR, Sastry KS and Rao DV: On the equivalent dose for Auger electron emitters. Radiat Res *134*: 71-78, 1993.

28 Mariani G, Bodei L, Adelstein SJ and Kassis AI: Emerging roles for radiometabolic therapy of tumors based on Auger electron emission. J Nucl Med *41*: 1519-1521, 2000.

29 Chen P, Cameron R, Wang J, Vallis KA and Reilly RM: Antitumor effects and normal tissue toxicity of ^{111}In-labeled epidermal growth factor administered to athymic mice bearing epidermal growth factor receptor-positive human breast cancer xenografts. J Nucl Med *44*: 1469-1478, 2003.

30 Tseng YL, Hong RL, Tao MH and Chang FH: Sterically stabilized anti-idiotype immunoliposomes improve the therapeutic efficacy of doxorubicin in a murine B-cell lymphoma model. Int J Cancer *80*: 723-730, 1999.

31 Lee WC, Hwang JJ, Tseng YL, Wang HE, Chang YF, Lu YC, Ting G, Whang-Peng J and Wang SJ: Therapeutic efficacy evaluation of ^{111}In-VNB-liposome on human colorectal adenocarcinoma HT-29/*luc* mouse xenografts. Nucl Instrum Meth A *569*: 497-504, 2006.

32 Li SD and Huang L: Pharmacokinetics and biodistribution of nanoparticles. Mol Pharm *5*: 496-504, 2008.

33 Chang CH, Wang HE, Wu SY, Fan KH, Tsai TH, Lee TW, Chang SR, Liu RS, Chen CF, Chen CH and Fu YK: Comparative evaluation of FET and FDG for differentiating lung carcinoma from inflammation in mice. Anticancer Res *26*: 917-925, 2006.

34 Massoud TF and Gambhir SS: Molecular imaging in living subjects: seeing fundamental biological processes in a new light. Genes Dev *17*: 545-580, 2003.

35 Chang CH, Jan ML, Fan KH, Wang HE, Tsai TH, Chen CF, Fu YK and Lee TW: Longitudinal evaluation of tumor metastasis by an FDG-microPet/microCT dual-imaging modality in a lung carcinoma-bearing mouse model. Anticancer Res *26*: 159-166, 2006.

36 Torigian DA, Huang SS, Houseni M and Alavi A: Functional imaging of cancer with emphasis on molecular techniques. CA Cancer J Clin *57*: 206-224, 2007.

37 Weissleder R: Molecular imaging in cancer. Science *312*: 1168-1171, 2006.

38 Owens DE, 3rd and Peppas NA: Opsonization, biodistribution, and pharmacokinetics of polymeric nanoparticles. Int J Pharm *307*: 93-102, 2006.

39 Liu D, Mori A and Huang L: Role of liposome size and RES blockade in controlling biodistribution and tumor uptake of GM1-containing liposomes. Biochim Biophys Acta *1104*: 95-101, 1992.

40 Levchenko TS, Rammohan R, Lukyanov AN, Whiteman KR and Torchilin VP: Liposome clearance in mice: the effect of a separate and combined presence of surface charge and polymer coating. Int J Pharm *240*: 95-102, 2002.

41 Zhang JS, Liu F and Huang L: Implications of pharmacokinetic behavior of lipoplex for its inflammatory toxicity. Adv Drug Deliv Rev *57*: 689-698, 2005.

42 Gregoriadis G: Engineering liposomes for drug delivery: progress and problems. Trends Biotechnol *13*: 527-537, 1995.

43 Ponce AM, Vujaskovic Z, Yuan F, Needham D and Dewhirst MW: Hyperthermia-mediated liposomal drug delivery. Int J Hyperthermia *22*: 205-213, 2006.

Received December 16, 2008
Revised February 24, 2009
Accepted April 2, 2009